

## Amelioration of neuropilin-1 and RAGE/matrix metalloproteinase-2 pathway-induced renal injury in diabetic rats by rosuvastatin

Rabia Nabi<sup>1</sup>, Sahir Sultan Alvi<sup>1</sup>, Sultan Alouffi<sup>2</sup>, Saif Khan<sup>3</sup>, Adnan Ahmad<sup>1</sup>, Mahvish Khan<sup>4</sup>, Saheem Ahmad<sup>2</sup> and M. Salman Khan<sup>1,\*</sup>

<sup>1</sup>IIRC-5, Clinical Biochemistry and Natural Product Research Lab, Department of Biosciences, Integral University, Lucknow, 226026, U.P., India

<sup>2</sup>Department of Clinical Laboratory Sciences, College of Applied Medical Sciences, University of Hail, Saudi Arabia

<sup>3</sup>Department of Basic Dental Sciences, College of Dental Sciences, University of Hail, Hail, Kingdom of Saudi Arabia

<sup>4</sup>Department of Biology, College of Science, University of Hail, Hail, Kingdom of Saudi Arabia

\*Corresponding author: mskhan@iul.ac.in

Received: March 16, 2021; Revised: April 22, 2021; Accepted: April 24, 2021; Published online: May 31, 2021

**Abstract:** Advanced glycation end-products (AGEs) induce the production of reactive oxygen species (ROS) and extra cellular matrix (ECM) degradation via suppression of neuropilin-1 (NRP-1) and interaction with AGE-receptors (RAGE). This study aimed to reveal whether modulation of NRP-1 by rosuvastatin (RT) prevents AGE-induced renal injury via targeting RAGE/matrix metalloproteinase-2 (MMP-2) signaling in diabetic rats. Treatment with RT ameliorated the altered level of markers of glycemic control, renal injury, cholesterol, triglyceride (TG) and hepatic HMG-CoA reductase activity; the level of circulatory carboxymethyl-lysine (CML) and the accumulation of fluorogenic-AGEs in renal tissue was reduced; the expression of renal NRP-1, a checkpoint target, was stimulated; the transcription of RAGE, NF $\kappa$ B-2, TGF- $\beta$ 1 and MMP-2 was suppressed; the circulatory carbonyl content (CC) and paraoxonase-1 (PON-1) activity was ameliorated, and renal histopathological features were attenuated as evidenced by improved glomerular appearance, Bowman's space and abundant podocytes in kidneys. In conclusion, RT exhibited the potential to counteract diabetes and AGE-induced renal pathologies via stimulation of NRP-1, suppression of RAGE, and of genes responsible for ECM disintegration (MMP-2) and the inflammatory response (NF $\kappa$ B-2).

**Keywords:** rosuvastatin; neuropilin-1; AGE/RAGE-signaling; carboxymethyl-lysine; fluorogenic AGEs

## INTRODUCTION

Diabetes mellitus (DM), a critical global health concern, has been correlated to long-term macro- and microvascular disorders, particularly diabetic nephropathy (DN) and accelerated atherosclerotic cardiovascular disease (ASCVD) [1]. The pathogenesis of DN affects up to 40% of cases with type-2 DM and is assumed to be the major determinant of end-stage renal disease [2,3]. The pathogenesis of DN is initiated by the deposition of the glomerular basement matrix, mesangial expansion, renal fibrosis with glomerulosclerosis and podocyte death that ultimately cause renal failure [1,4,5]. There are several risk factors that lead to the initiation and advancement of DN. Persistently unmanaged glycemic

control-induced generation of advanced glycation end products (AGEs) has recently been established as a key mediator that triggers diabetic kidney disease [1,2,6,7]. AGE-associated complications under hyperglycemia in DN are primarily influenced by the interaction of circulatory and tissue AGEs with their receptors (RAGE), which activate distinct signaling pathways [1,7-9]. The level of plasma AGEs, including pentosidine and carboxymethyl-lysine (CML) and their soluble receptors, has been strongly correlated with the severity of diabetic microvascular complications, including DN and renal fibrosis [10].

The interaction of AGE with RAGE also triggers oxidative stress and inflammatory cascades in distinct renal cells resulting in the loss of renal architecture

and functions associated with tubular injury [7,11]. Apart from RAGE and its transcriptional activator, nuclear factor- $\kappa$ B (NF- $\kappa$ B), the matrix metalloproteinase-2 (MMP-2), also significantly contributes to DN via disintegration of collagen (both type-I and type-IV), proteoglycans and laminin, the major components of renal tissues [7,12]. A recent study has established that exposure to low-density lipoprotein (LDL)-AGEs significantly upregulated the level of MMP-2 and its transcriptional regulator, transforming growth factor- $\beta$ 1 (TGF- $\beta$ 1) in HEK-293 cells [7]. TGF- $\beta$ 1 is a multifunctional cytokine that participates in diabetic kidney dysfunction by facilitating the buildup of extracellular matrix (ECM) counterparts in the glomeruli and other target sites of MMP-2 [13-15], and overexpression of TGF- $\beta$ 1 has been reported in LDL-AGEs-exposed HEK-293 cells, pointing to its role in the establishment of DN [7].

Besides the contributing role of RAGE in DN, another transmembrane receptor, neuropilin-1 (NRP-1) that is expressed in distinct cells, including renal cells, regulates discrete signaling pathways, particularly those associated with the AGE-RAGE axis, and protects against renal abnormalities [16]. Recently, we showed that exposure to a high level of low density lipoprotein (LDL)-AGE significantly downregulates NRP-1 transcription in HEK-293 cells [7]. AGE-directed cardiovascular complications are critically affected by the functionality of HMG-CoA reductase (HMG-R) [1,7], an enzyme involved in hepatic cholesterol synthesis and lipid homeostasis [17-19]. In light of this knowledge, targeting hyperglycemia, cholesterol homeostasis, the formation of AGEs, oxidative stress and AGE-RAGE-associated signaling has now been established as a promising therapeutic target in DN management.

Although the implication of aminoguanidine, the standard inhibitor of *in-vitro* AGE formation [11], has exhibited adverse effects in different experimental settings, such as cell culture, animal model studies and human clinical trials in diabetic kidney disease [7,20], the development of an anti-AGE therapeutic approach remains open for the management of DN. Rosuvastatin (RT) is one of the most preferred modulators of cholesterol homeostasis because of its ability to block hepatic HMG-R [1,11]. A recent report demonstrated that RT decreases the glucose level via enhanced insulin sensitivity and glucose transport in adipocytes as well as

in cholesterol-fed mice [21]. It also increases insulin secretion dose-dependently in NS-1 832/13 cells [22]. We demonstrated that RT exhibits a strong *in vitro* antiglycation effect and also protects HEK-293 cells against LDL-AGE-stimulated reactive oxygen species (ROS) generation and AGE-RAGE-associated signaling [7,11]. Except for our recent *in vitro* findings, there is no report that documents the *in vivo* effect of RT on AGE-induced diabetic microvascular complications. Therefore, in a continuation of our research findings, the current *in vivo* study was undertaken to examine whether the modulation of NRP-1 by RT prevents AGE-induced renal injury via targeting distinct biochemical markers, including NRP-1 expression and subsequent ECM regeneration, and AGE-RAGE cross-talk in the experimental diabetic rat model.

## MATERIALS AND METHODS

### Experimental animals

Male Sprague-Dawley rats (0.15-0.2 kg) were obtained from CDRI-Lucknow, India and were familiarized to the animal house settings for seven days (21-25°C). The ethical concerns for this study were cleared by the University IAEC, Integral University (IU/BioTech/project/IAEC/17/02) and was carried out according to the principles of animal experimentation issued by the Government of India.

### Drugs, reagents and kits

The biochemical kits for the estimation of creatinine, total cholesterol (TC) and triglycerides (TG) were purchased from Agappe Diagnostic Ltd., Chennai, India; the high-density lipoprotein (HDL) kit was obtained from the Autospan gold liquid kit, Surat-Gujrat, India. The ELISA kit for quantitative determination of plasma CML was purchased from Bioassay Technology Laboratory Co. Ltd., Shanghai, China; rat insulin and microalbumin ELISA kits were supplied by Elabscience® Ltd., USA. RT and glibenclamide (GB) were purchased from Sigma Aldrich Co., USA. Streptozotocin (STZ) was obtained from Sisco Research Laboratories Pvt. Ltd., Mumbai, India. The GenX HbA1c automated immunoassay kit was supplied by Proton Biologicals India Pvt. Ltd., India. The

remaining chemicals/reagents/kits used for molecular assays were of analytical grade unless mentioned in the respective methodology sections.

### **In vivo experimental design**

#### **STZ, RT and GB preparation**

Fresh STZ (60 mg/kg b.w. of rat) was dissolved in citrate buffer (pH 4.5) as reported earlier [23,24]. The doses of RT [25] and the reference drug GB (10 mg/Kg B.W./rat/day) were prepared in 10% DMSO as per recent reports [23,24].

### **Experimental diabetes**

The animals were assigned to four groups and DM was induced as described [23,24]. Briefly, fasted animals were injected intraperitoneally (i.p.) with freshly prepared STZ, except the control group in which the rats received only citrate buffer as the STZ vehicle. Fasting blood glucose (FBG) was determined after 72 h of STZ injection using an Accu-Chek glucometer. Rats with FBG  $\geq 230$  mg/dL were designated as diabetic and appropriate for the therapeutic intervention study. The induction and treatment plan are summarized in Supplementary Table S1.

### **Collection and preparation of blood, plasma and tissues for biochemical and molecular assays**

Whole blood was collected by cardiac puncture in tubes containing the anticoagulant agent heparin, and processed as described to obtain plasma [19,26]. Hepatic and renal tissues were also rapidly excised, washed with chilled saline and stored at -20°C until further biochemical and molecular assays.

### **Biochemical assays**

#### **Determination of blood glucose and HbA1c level**

The level of FBG was measured by an enzymatic "Autospan kit" following the manufacturer's instructions as described earlier [23]. The level of HbA1c was determined using a GenX HbA1c automated immunoassay kit supplied by Proton Biologicals India Pvt. Ltd., India. The assay principle was based on the

direct interaction of antigen and antibody, and the percentage of HbA1c was calculated by measuring the absorbance of lyophilized calibrators at 660 nm with an Eppendorf BioSpectrophotometer [23].

### **Estimation of plasma insulin by ELISA**

The estimation of plasma insulin was performed with a high sensitivity and high specificity rat insulin ELISA Kit, Elabscience Ltd., USA. Briefly, 100 µL of either standard/calibrator or plasma samples were added to respective wells in the ELISA plates that were precoated with rat insulin specific antibodies (Abs) except the blank. Following incubation at 37°C for 90 min and aspiration of the reaction mixture, 100 µL of biotinylated Ab for rat insulin was added and left at 37°C for 60 min. Subsequently, the plate was washed three times and incubated with 100 µL of HRP conjugate for 30 min at 37°C and washed five times after decanting/aspiring the solution from each well. Appropriate volumes of the substrate reagent (90 µL) and stop solution (50 µL) were added to each well and the intensity of the formed chromogenic product was determined on an iMark™ Bio-Rad, USA microplate absorbance reader.

### **Estimation of circulatory microalbumin by ELISA**

The estimation of plasma microalbumin was performed in accordance with a high sensitivity and high specificity rat microalbumin ELISA Kit, Elabscience Ltd., USA. The methodology was the same as described for the quantification of rat insulin, while the micro-ELISA plate was precoated with rat microalbumin-specific antibody.

### **Determination of plasma TC, TG, and lipoprotein levels**

Plasma TC level was estimated by the Cholesterol LiquiCHEK™ enzymatic kit from AGAPPE, India [19]. Similarly, the TG level was estimated using the Triglycerides LiquiCHEK™ enzymatic kit from AGAPPE, India [26]. The HDL-C level was estimated by the Autospan Reagents, Span Diagnostics, Gujarat, India. The level of VLDL-C was obtained by dividing the TG values of the respective groups by 5 [19]. Plasma LDL-C was prepared and quantified following the standard method [19,27]. The level of non-HDL-C

was achieved by deducting the HDL-C level from the TC level [19,26].

### Plasma creatinine estimation

Plasma creatinine was assayed by the LiquiCHEK™ enzymatic creatinine assay kit supplied by AGAPPE, India. The assay principle was based on the enzymatic actions of creatininase, creatinase and sarcosine oxidase to convert creatinine into H<sub>2</sub>O<sub>2</sub>, which subsequently reacted with 4-aminoantipyrine and N-ethyl-N-(2-hydroxy-3-sulfopropyl)-m-toluidine to give a colored quinone product that was measured at 546 nm against the blank.

### Plasma FRAP, PON-1 and carbonyl content assay

The plasma ferric reducing antioxidant power (FRAP) was estimated by the standard protocol [28] with slight optimization [19,26]. The activity of paraoxonase-1 (PON-1) in plasma was assessed by the standard protocol and CH<sub>3</sub>COOC<sub>6</sub>H<sub>5</sub> was used as the PON-1 substrate [19,29]. The plasma carbonyl content (CC), the product of protein glycation/oxidation, was estimated using the 2,4-dinitrophenylhydrazine (DNPH) assay [11,30]. The OD was recorded at 360 nm and the CC level was calculated by applying a MEC of 22 x 10<sup>3</sup> M<sup>-1</sup> cm<sup>-1</sup> [30].

### Measurement of plasma CML level via ELISA

The level of plasma CML, one of the most characterized AGEs, was quantified using the CML ELISA kit. Briefly, either 40 µL of sample and 10 µL of biotinylated Rat anti-CML Ab or 50 µL of the standard (without rat anti-CML Ab) was added to the ELISA plate which was precoated with rat CML Abs, followed by the addition of 50 µL of streptavidin-HRP to both sample and standard wells. The plate was incubated and washed repeatedly, and 50 µL of each substrate A and B were added and incubated. The color intensity was read at 450 nm after addition of stop solution using a Bio-Rad plate reader.

### Estimation of renal fluorescent AGEs

The level of fluorescent AGEs in the kidney homogenate was quantified as described [31]. Briefly, a

portion of the kidney was homogenized in 0.25 M sucrose and extracted [32]. Soluble proteins in the kidney homogenate were determined by the Bradford method [33], and the concentration of the proteins was adjusted to 1 mg/mL; the level of fluorescent AGEs was assessed using an Agilent (US) spectrofluorometer with a  $\lambda_{\text{Ex}}$  of 370 nm and a  $\lambda_{\text{Em}}$  range of 380-550 nm.

### Liver homogenate preparation

One g of washed and ice-cold liver was homogenized with 0.1 M chilled phosphate buffered saline (PBS) in a homogenizer. The obtained homogenized suspension was centrifuged at 1000 rpm for 10 min at 4°C, and a portion of the homogenate was aliquoted and stored at -20°C.

### Assay of HMG-CoA reductase (HMG-R) activity

HMG-R is the key enzymatic target in cardiovascular pharmacology, and is the central enzyme in the synthesis of cholesterol [17,34]. The activity of hepatic HMG-R was estimated by following standard protocols [19,26]. In brief, the appropriate volume of liver homogenate was added to 9 mL 0.1% saline arsenite followed by the addition of 5% perchloric acid. After incubation and centrifugation, a 1-mL supernatant was mixed with 500 µL of 1 M of alkaline hydroxylamine hydrochloride for the determination of mevalonate and HMG-CoA. Then, 1.5 mL of 616 mM FeCl<sub>3</sub> was added to the resulting mixture, incubated and read at 540 nm in an Eppendorf BioSpectrophotometer.

### Isolation of RNA

RNA was isolated from kidney tissues of all groups using TRIzol™ reagent (Invitrogen, USA) as described [19]. The RNA pellet was dissolved in diethyl pyrocarbonate (DEPC) water and quantified by nanodrop.

### cDNA synthesis

The cDNA was produced using the Applied Biosystems™ cDNA Reverse Transcription Kit (Thermo Fisher Sci., India). The reaction mixture (20 µL) containing 2000 ng of RNA and Master Mix

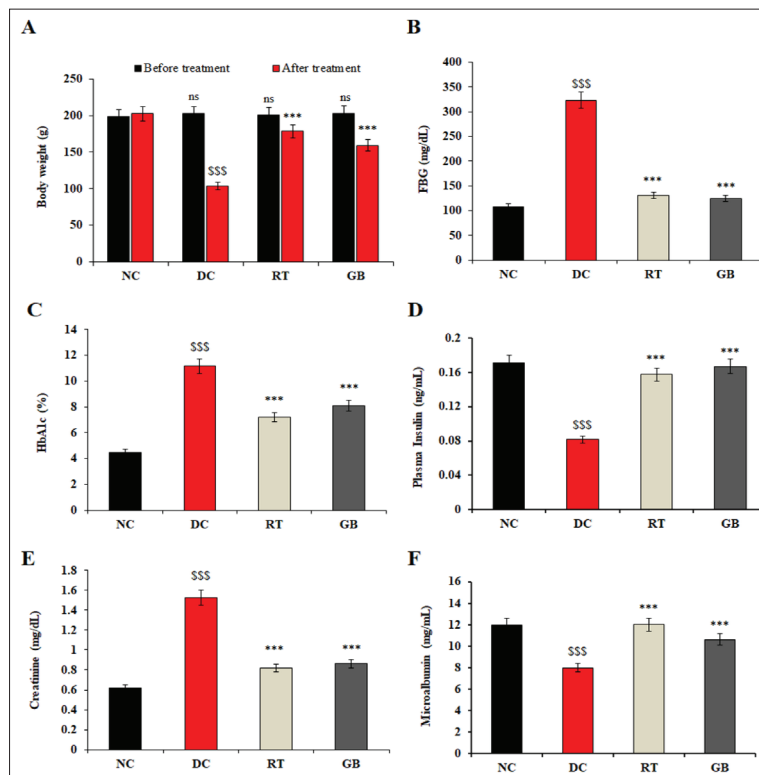


**Fig. 1.** A – Impact of RT treatment on the body weight of STZ-induced diabetic rats. Values (g) are expressed as the mean±SEM of three determinants. No significant difference in the body weight of rats among different groups was reported before treatment (<sup>ns</sup>P>0.05). Significant from NC at <sup>\$\$\$</sup>P<0.001 (after treatment). Significant from DC at <sup>\*\*\*</sup>P<0.001 (after treatment). B – RT reduces the blood glucose level in diabetic rats. Values (mg/dL) are the mean±SEM from three independent determinations from each group. C – RT lowers the level of glycated hemoglobin (HbA1c) in diabetic rats. Values (% HbA1c) are the mean±SEM from three independent assays of each group. D – RT elevates the insulin level in diabetic rats after 4 weeks of treatment. Values (ng/mL) are the mean±SEM from three independent assays of each group. E – RT improves plasma creatinine concentration in diabetic rats. Values (mg/dL) are expressed as the mean±SEM from three independent assays of each group. F – RT increased circulatory microalbumin in diabetic rats. Values (mg/mL) are the mean±SEM. Stats for panels B-F: significant from NC rats at <sup>\$\$\$</sup>P<0.001; significant from DC rats at <sup>\*\*\*</sup>P<0.001. NC – normal control; DC – diabetic control; RT – rosuvastatin-treated rats (10 mg/kg b.w./rat/day); GB – glibenclamide-treated rats (10 mg/kg b.w./rat/day).

was subjected to thermocycling with the following program: 25°C for 10 min, 37°C for 120 min, 85°C for 5 min [19,33].

#### Gene expression (qRT-PCR) analysis

Gene-specific oligonucleotide primers were customized using Primer Express Software-3.0.1 (Supplementary Table S2). qRT-PCR analysis was

performed using 10 µL SYBR®Premix Ex Taq™ II (TliRNaseH Plus, DSS Takara, India), 1 µL primers for each gene, 5 µL of cDNA and RNase free water. qRT-PCR analysis was run on a BioRadCFX 96™ Real-Time System with the following cycle profiles: 10 min at 95°C for activation (1 cycle), 15 s at 95°C (40 cycles), 1 min annealing at 60°C, extension at 72°C for 45 s. The difference in gene expression were determined by the  $2^{-\Delta\Delta Ct}$  protocol and expressed as the fold-change against  $\beta$ -actin [7,26].

#### Histopathological investigations

Kidney sections from each group were fixed in 10% formalin and paraffin blocks were prepared, sectioned, stained with Ehrlich's hematoxylin and eosin (H&E) and observed under the microscope [23,24].

#### Statistical analysis

Biochemical and molecular assays were performed in triplicate and the data were expressed as the mean±SEM. The variables were subjected to one-way analysis of variance (ANOVA), followed by the post hoc Tukey-Kramer test using GraphPad Prism software (Ver 4.02) as described previously [19,26,33].

## RESULTS

#### Rosuvastatin maintains body weight in experimental diabetic rats

The weight of DC rats was significantly reduced compared to NC rats (Fig. 1A). Administration of RT to diabetic rats for the designated duration caused a marked improvement in body weight when compared to untreated DC rats. Treatment with GB also revealed an almost similar gain in body weight when compared to untreated DC rats.

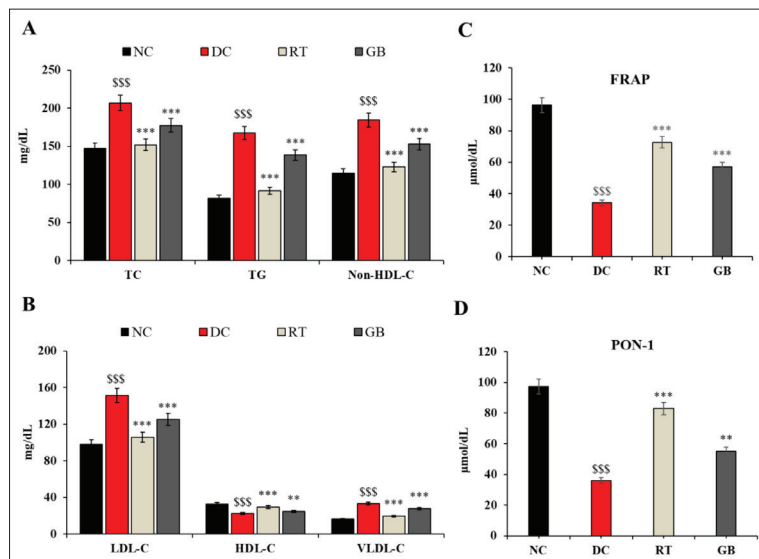


**Fig. 2.** A, B – RT treatment restores plasma cholesterol and carrier lipoproteins in diabetic rats. Values (mg/dL) are the mean±SEM from three determinants. C – Administration of RT restores plasma FRAP activity in diabetic rats. Values ( $\mu$ mol/dL) are the mean±SEM. D – administration of RT restores plasma PON-1 activity in diabetic rats. Values ( $\mu$ mol/dL) are the mean±SEM from three determinations of pooled plasma from each group. Stats for panels A-D: significant from NC rats at \*\*\*P<0.001; significant from DC rats at \*\*\*P<0.001; significant from DC rats at \*\*P<0.01.

### Rosuvastatin ameliorates the markers of glycemic control in STZ-induced diabetic rats

Experimental diabetes caused a significant increase in FBG concentration from 108.2 to 323.3 mg/dL in untreated DC rats compared to NC rats. However, administration of RT to diabetic rats for 4 weeks decreased the FBG level when compared to DC rats. The standard drug GB also caused a significant reduction in FBG concentration when compared to DC rats (Fig. 1B). The level of HbA1c, an index for persistently elevated mean blood glucose concentration, was significantly elevated from 4.51% in NC rats to 11.16% in DC rats. However, subsequent treatment with RT for 4 weeks caused a decrease in the concentration of HbA1c up to 7.2 % when compared to DC rats. Similarly, administration of GB also decreased the concentration of HbA1c (Fig. 1C). As shown in Fig. 1D, the STZ challenge resulted in the decline of the plasma insulin level in diabetic rats, which was markedly improved after they were administered with RT. The treatment with GB also improved the plasma insulin level in STZ-challenged diabetic rats.

### RT diminishes plasma creatinine and microalbumin levels in experimental hyperglycemia

As shown in Fig. 1E, the concentration of plasma creatinine was significantly increased in diabetic rats and subsequent treatment with RT markedly decreased the plasma creatinine level. GB also caused a significant decline in plasma creatinine concentration in diabetic rats when compared to matching DC rats. In contrast, a diminished level of plasma microalbumin was observed in DC rats when compared to matching NC rats. However, oral administration of RT significantly ( $P<0.001$ ) improved the level of circulatory microalbumin. The treatment with GB also significantly raised plasma microalbumin (Fig. 1F).

### RT maintains plasma cholesterol and carrier lipoproteins in diabetic rats

The results from our interventional study showed that plasma TC, TG and non-HDL-C content were significantly increased, from 147.3 mg/dL to 207.05 mg/dL, from 81.72 mg/dL to 167.7 mg/dL and from 114.65 to 184.74 mg/dL in DC rats, respectively, when compared to NC rats. Administration of RT led to a marked decline in circulatory TC, TG and Non-HDL-C by 26.51%, 45.15% and 33.51%, respectively, whereas the treatment with GB showed a decline in the level of TC, TG and non-HDL-C by 23.26%, 17.35%, and 17.20%, respectively, when compared to untreated DC rats (Fig. 2A). In addition, the LDL-C, HDL-C and VLDL-C were also altered in DC rats by +53.80%, -31.67% and +105.26%, respectively, when compared to NC rats; RT administration markedly altered their levels by -30.08%, +33.03% and -41.72% in diabetic rats, respectively, with GB also improving the level of these markers (Fig. 2B).

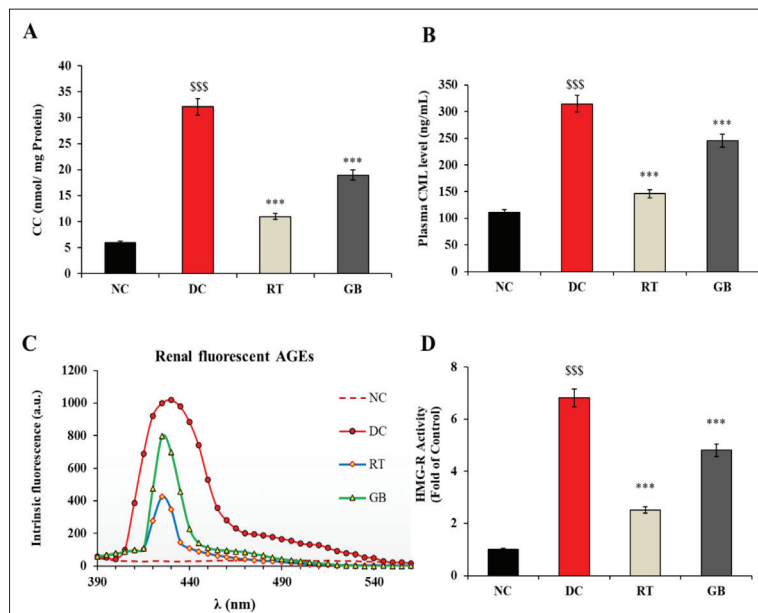


**Fig. 3.** A – Treatment with RT diminishes the level of plasma protein bound CC in STZ-induced diabetic rats. Values (nmol/mg protein) are the mean $\pm$ SEM from three determinations. B – administration of RT significantly reduces the level of plasma AGEs (CML). Values (ng/mL) are the mean $\pm$ SEM from three determinations of pooled plasma from each group. C – RT prevents the accumulation of fluorescent AGEs in kidney of diabetic rats. Determination of AGEs in the kidney homogenate was based on the spectrofluorimetric detection of fluorescent AGEs. D – RT significantly inhibits hepatic HMG-R activity. Values are the mean $\pm$ SEM from triplicate assays of pooled liver homogenates from each group. Stats for panels A, B and D: significant from NC rats at \$SS\$P<0.001; significant from DC rats at \*\*\*P<0.001.

#### RT enhances plasma FRAP and HDL-associated PON-1 activities

The data from our interventional study showed that experimental diabetes led to diminished plasma FRAP activity in DC rats when compared with NC rats. The treatment with RT and GB markedly elevated plasma FRAP values by 112.47% and 66.56%, respectively, when compared to matching untreated DC rats (Fig. 2C). In contrast, the activity of HDL-associated PON-1 in the plasma of DC rats was also diminished; treatments with RT and GB significantly increased plasma PON-1 activity by 130.08% and 52.74%, respectively, when compared to DC rats (Fig. 2D).

#### RT restores the protein bound carbonyl content in STZ-induced diabetic rats

Protein bound CC, a global biomarker of protein oxidation, was assessed to determine the protein carbonyl

groups in plasma [11,30]. The data from our *in vivo* experiment showed that the level of protein-bound CC was markedly elevated from 5.99 to 32.09 nmol/mg protein in DC rats. However, treatment with RT markedly diminished the level of CC when compared to untreated DC rats. Moreover, the GB treatment also reduced the level of CC in diabetic rats but to a lesser degree than RT (Fig. 3A).

#### RT reduces plasma CML-AGEs in STZ-induced diabetes

Persistent hyperglycemia is linked with increased formation of AGEs [1]. Examination of the level of CML-AGEs in plasma revealed that the level of plasma CML-AGEs was increased from 110.94 to 314.83 ng/mL in experimental diabetic rats. However, treatment with RT effectively ameliorated the increase in plasma CML-AGEs in diabetic rats when compared to matching DC rats. GB-treated diabetic rats also displayed restoration in plasma CML-AGEs when compared to DC rats (Fig. 3B).

#### RT reduces the accumulation of AGEs in kidney of diabetic rats

Enhanced levels of circulatory AGEs lead to their subsequent accumulation in different tissues, including the kidney [1,7]. The degree of AGE accumulation in the kidney homogenate was determined by fluorescence spectroscopy. Fluorescent intensity (FI) was found to be increased by 96.94% in DC rats, when compared with the FI of the kidney homogenate from NC rats, which indicates that STZ-induced diabetes led to increased levels of fluorescent AGEs in the kidney homogenate. However, the administration of RT significantly reduced the emission of AGE-specific fluorescence; the standard drug GB also restored AGE-specific fluorescence when compared with matching untreated DC rats (Fig. 3C).

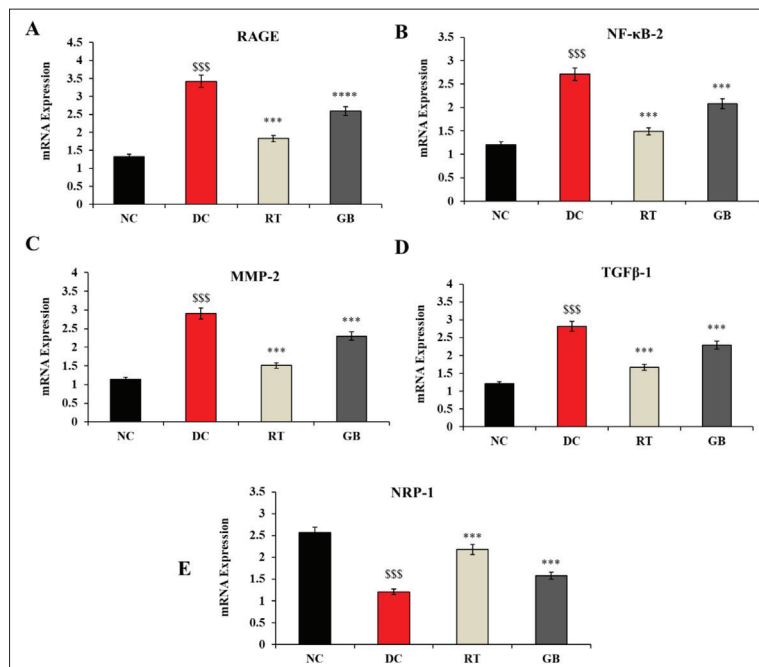


**Fig. 4.** Treatment with RT significantly modulates renal AGE-RAGE signaling in STZ-induced diabetic rats. **A, B** – RT downregulates renal RAGE and NF $\kappa$ B-2 transcription, respectively. Values are the mean $\pm$ SEM. **C, D** – RT suppresses renal MMP-2 and TGF $\beta$ -1 transcription, respectively. Values are the mean $\pm$ SEM. **E** – RT upregulates renal NRP-1 mRNA expression. Values are expressed as the mean $\pm$ SEM. Stats for panels A-E: significant from NC rats at \*\*\*P<0.001; significant from DC rats at \*\*\*P<0.001.

### RT inhibits hepatic HMG-R activity in diabetic rats

HMG-R activity was significantly elevated 6.82-fold in DC rats. However, intervention with RT apparently lowered HMG-R activity to a 2.51-fold increase with respect to the control. GB treatment also decreased hepatic HMG-R activity in diabetic rats to a 4.81-fold increase with respect to the control when compared to untreated DC rats, but the decrease in HMG-R activity caused by GB treatment was not as much as that observed in RT-treated rats (Fig. 3D).

### RT downregulates renal transcription of RAGE and NF $\kappa$ B-2 in diabetic rats

The data from the current report show that diabetes led to a significant upregulation of renal RAGE mRNA expression. Moreover, the treatment with RT markedly downregulated RAGE mRNA expression when compared to DC rats (to a 1.83-fold increase above

the control level). The reference drug GB also exhibited suppression of RAGE mRNA expression (to a 2.59-fold increase above the control level) when compared to matching DC rats (Fig. 4A). In contrast, the expression of NF $\kappa$ B-2, the transcription factor associated with RAGE expression, was found to be upregulated in diabetic rats (2.71-fold above the control level). However, administration of RT to diabetic rats significantly suppressed NF $\kappa$ B-2 expression (to a 1.49-fold increase above the control level). Treatment with GB also suppressed NF $\kappa$ B-2 mRNA (to a 2.08-fold increase above the control level) (Fig. 4B).

### RT downregulates renal MMP-2 and TGF $\beta$ -1 expression in diabetic rats

The findings of gene expression analysis revealed that the MMP-2 was significantly upregulated (2.91-fold higher than the control) in STZ-induced diabetic rats. Treatment with RT markedly suppressed MMP-2 transcription in diabetic rats (to a 1.51-fold increase above the control); treatment with GB produced a comparatively lower downregulation of MMP-2 mRNA (to a 2.30-fold increase above the control) (Fig. 4C).

Examination of the expression of TGF $\beta$ -1, the transcriptional inducer of MMP-2 in renal tissue that was assessed in all groups by qRT-PCR analysis, revealed that the transcription of TGF $\beta$ -1 mRNA was significantly upregulated (2.82-fold relative to the control level) in STZ-induced diabetic rats, and when compared with the renal TGF $\beta$ -1 mRNA levels in matching NC rats (1.21-fold relative to the control). Treatment with RT significantly diminished the expression of TGF $\beta$ -1 mRNA levels (to a 1.66-fold increase above the control level). In contrast, the administration of GB caused a lower decrease in the degree of amelioration in the expression of TGF $\beta$ -1 mRNA (a 2.29-fold increase above the control level) (Fig. 4D).

### RT upregulates the expression of renal NRP-1 mRNA in diabetic rats

Analysis of the expression of NRP-1 in renal tissues revealed that NRP-1 expression was significantly down-regulated in DC rats (to a 1.21-fold increase above the control level) when compared to NC rats (which exhibited a 2.56-fold increased level compared to the control). Administration of RT significantly stimulated NRP-1 transcription (2.18-fold above the control level) in diabetic rats, whereas the treatment with GB augmented NRP-1 transcription to a comparatively lesser extent (Fig. 4E).

### RT maintains the renal histopathological features in experimental diabetes

Histopathological examination of the kidney after 4 weeks of administration of RT and GB to STZ-induced diabetic rats revealed that NC rats had normal glomerular lobules with normal Bowman's space and an abundant podocyte count (Fig. 5). In contrast, STZ-induced diabetes accompanied by oxidative stress and AGE-RAGE signaling was characterized by degenerative changes in kidney, including enlarged Bowman's spaces and smaller podocyte counts in DC rats. The administration of RT showed marked normalization of Bowman's space, glomerular lobule appearance and podocyte abundance, when compared to DC rats; GB treatment also normalized the Bowman's space, glomerular lobules and podocyte count. No other significant pathology was observed in either RT- or GB-treated rats.

### DISCUSSION

Persistent hyperglycemia in DM, if left untreated, contributes to the initiation, progression and development of distinct secondary complications of diabetes via the formation and accumulation of AGEs [1,9]. Moreover, inhibition of AGE formation, maintenance of redox homeostasis and lipid metabolism and regulation of RAGE expression and associated signaling are considered to be the most promising therapeutic strategies in diabetes and related complications [7,30]. Recently, we showed that RT potentially inhibits *in vitro* protein (bovine serum albumin and LDL) AGE formation as

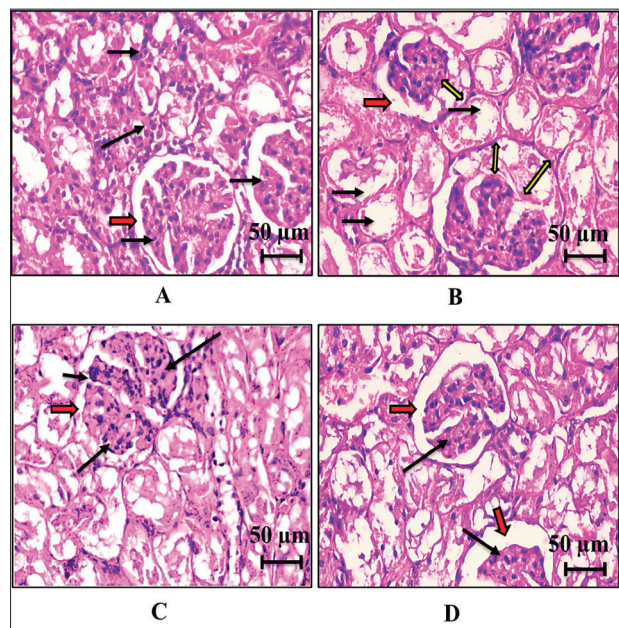


**Fig. 5.** RT maintains renal histopathological features in experimental diabetic rats. Histopathological study of kidney was performed after 4 weeks of administration of RT and GB to STZ-induced diabetic rats. **A** – kidney micrograph from NC rats showing normal glomerular appearance, normal Bowman's space (thick red arrows) and abundant podocytes (thin black arrows). **B** – kidney micrograph from DC rats showing abnormal glomerular appearance with glomerulosclerosis (thick yellow arrows), enlarged Bowman's space (thick red arrows), and reduced podocyte count (thin black arrows). **C** – Kidney micrograph from RT-treated rats showing normal glomerular appearance, normal Bowman's space (thick red arrows) and abundant podocytes (thin black arrows). **D** – kidney micrograph from GB-treated rats with normal glomerular appearance, normal Bowman's space (thick red arrows) and abundant podocytes (thin black arrows).

well as LDL-AGE-triggered AGE-RAGE signaling in HEK-293 cells [7,11]. Other studies in animal models and human clinical trials also showed the antidiabetic potential of RT, but to the best of our knowledge, there are no reports that present mechanistic insights into the role of RT in attenuating diabetes-mediated renal pathologies. Herein, we assessed the therapeutic impact of RT in attenuating STZ-induced diabetes and renal pathologies via the targeting of distinct mechanisms, in particular the glycemic and redox status, formation of AGEs, NRP-1 expression and RAGE-associated signaling.

STZ is an acknowledged compound used for the induction of experimental diabetes in animal models as it causes DNA damage in pancreatic  $\beta$ -cells leading

to impaired insulin secretion and cell death [23,24,35]. The data from our study revealed that DC rats showed increased FBG levels due to STZ-induced DNA damage in pancreatic  $\beta$ -cells and compromised plasma insulin level. The elevated FBG level was decreased upon oral administration of RT and GB, which could be attributed to the protective effects of these pharmaceutical agents against pancreatic DNA damage, as well as regeneration of  $\beta$ -cells that ultimately modulated insulin secretion, observed as the amelioration of the level of plasma insulin in both RT- and GB-treated rats. These effects of RT and GB on FBG and plasma insulin in experimental diabetic rats are expected as in other reports the hypoglycemic effects of both compounds was demonstrated [23,24,36]. HbA1c is a highly sensitive indicator of glycemic control [24,37]. We also reported a significant rise in HbA1c in DC rats that may be attributed to the increased glycosylation of hemoglobin (Hb) due to the persistently elevated blood glucose levels. However, administration of RT markedly reduced the level of HbA1c, which could be due to the RT-mediated improvement in blood sugar control as well as decreased interaction between blood sugar and Hb.

Elevated plasma creatinine is a well-known biomarker of the progression of diabetic nephropathy [38]. The glomerular filtration rate (GFR) in glomerulonephritis declines, which leads to reduced creatinine clearance and subsequent elevation in plasma creatinine level [39]. We also observed a substantial increase in plasma creatinine level in DC rats, which could be associated with increased protein degradation and reduced GFR. The administration of RT to diabetic rats markedly reduced the plasma creatinine level as compared to the DC group, which could be due to the increased renal clearance of circulatory creatinine. These results are strongly supported by a previously published report [40]. Similarly, the diminished level of serum microalbumin is a recognized early biomarker of DN [41,42]. We observed the reduction in plasma microalbumin level in DC rats that could be attributed to increased urinary microalbumin secretion under abnormal kidney functioning due to persistent hyperglycemia. However, the administration of RT and GB markedly improved the level of plasma microalbumin in diabetic rats and probably prevented urinary loss of microalbumin due to improved renal functioning. The observed level of

plasma microalbumin is in agreement with previous reports [15,43].

The pathophysiology of DN has been strongly linked with dyslipidemia [1,24,44]. In our *in vivo* study, TG and atherogenic lipoproteins (LDL-C) were significantly elevated in DC rats, which was attributed to increased hepatic HMG-R activity. Previous studies showed that experimental hyperglycemia leads to raised hepatic HMG-R activity in rats [23,24]. These alterations in the levels of TC, lipoproteins and TG were markedly ameliorated after 28 days of treatment of diabetic rats with RT. The attenuation achieved by RT administration is supported by the diminished hepatic HMG-R activity observed in our study. HMG-R inhibition produced by treatment with RT in diabetic rats is in agreement with studies that demonstrated pharmacological inhibition of HMG-R activity by other inhibitors [19,26,45]. The GB-treated group also exhibited restoration of altered lipid and lipoprotein levels, and these effects are consistent with a previous report [24], however, the reduction was much less than that caused by the RT treatment.

Diabetes is characterized by enhanced free radical generation, as well as by diminished activity of plasma HDL-associated PON-1 [46]. Our results show a decreased level of HDL-C as a result of decreased activity of plasma PON-1. Other studies also demonstrated compromised HDL-associated PON-1 activity in different animal models [19,26]. Administration of RT improved plasma PON-1 activity in diabetic rats and elevated plasma HDL-C. The improvement in PON-1 activity by RT treatment may also be associated with the decreased blood sugar concentration that ultimately protected HDL from glycation; HDL is linked with reduced PON-1 activity under the influence of oxidative stress [19,26,47]. In addition, the decreased level of FRAP in diabetic rats was also improved by the treatment with RT, and this could be attributed to the antioxidant potential of RT [7,11]. Increased production of free radicals in hyperglycemia results in the buildup of reactive carbonyl species (RCS), the global biomarker for the protein oxidation [11,30]. We also reported that the level of plasma protein-bound CC was markedly increased in experimental diabetes, however, repeated oral administration of RT significantly diminished the level of plasma CC in diabetic rats as a result of the potent antioxidant and antiglycation activities of RT;

RT was previously shown to exhibit shielding effects against D-ribose-triggered *in vitro* protein-bound CC generation, as well as AGE-stimulated ROS production in HEK-293 cells [7,11].

Exposure to reducing sugars induces glycation of different proteins, resulting in the formation of AGEs, ROS and RCS with a proclivity to irreversibly alter the structure of proteins and lipids and ultimately lead to severe renal complications [11,30,48]. Marked production of AGEs, particularly of CML and pentosidine, leads to their accumulation in different organs, including glomerular tissue, which can worsen renal complications [1,10,49]. In the same context, our results also showed that the levels of plasma CML and renal fluorescent AGEs were markedly elevated in diabetic rats. Oral administration of RT significantly decreased the level of plasma CML and reduced the accumulation of renal AGEs possessing intrinsic fluorescence in diabetic rats. These beneficial effects of RT on plasma as well as on the tissue level of AGEs could be ascribed to the potent antiglycation and antioxidant activities of RT that have already been described in our biochemical, biophysical and cell culture studies [7,11]. Thus, this is the first *in vivo* report on RT-mediated inhibition of different glycation markers, such as protein-bound CC, plasma CML and fluorescent AGEs, which provides strong support that RT possesses the potential to protect plasma proteins and renal tissue through the reduction in circulatory AGE formation in diabetes.

The molecular mechanism underlying the protective effects of RT in experimental diabetic rats was also assessed. Studies have established that AGE-RAGE interaction as the key mechanistic aspect of AGE-induced diabetic complications [1,9,10,50]. RAGE is expressed in different cells, including HEK-293, podocytes and proximal tubules of the kidney [7]. Our results also revealed increased RAGE transcription in renal tissue of diabetic rats. However, augmented expression of RAGE was markedly suppressed after treatment with RT. The suppression of RAGE expression by RT is in agreement with our previously published *in vitro* report in which we showed that RT significantly suppressed RAGE transcription in LDL-AGEs-challenged HEK-293 cells [7].

AGEs stimulate RAGE expression, and AGE-RAGE interaction triggers the expression of transcription

factor NF- $\kappa$ B [1,51,52]. The expression of renal NF- $\kappa$ B mRNA in DC rats was upregulated, and significantly downregulated in RT-treated diabetic rats, likely due to the decrease in AGE and ROS. TGF- $\beta$ 1, a major profibrotic cytokine, promotes renal interstitial fibrosis and matrix hypertrophy [13,15,53]. It has also been established that the accumulation of AGEs and AGE-RAGE interaction in renal and other cells is strongly related to increased renal TGF $\beta$ -1 expression [1,7]. Herein we observed significant elevation in TGF $\beta$ -1 mRNA in diabetic animals due to increased oxidative stress and AGE-RAGE interaction. Treatment of diabetic animals with RT significantly suppressed the expression of TGF $\beta$ -1, possibly achieved through its antioxidant activity, reduced level of AGEs, and reduced AGEs-RAGE signaling.

MMP-2 is considered to be a key target in the therapeutic management of DN due to its ability to affect the ECM in kidney tissues [7,15]. Augmented synthesis of MMP-2 mRNA and protein has been reported in response to hyperglycemia due to higher levels of AGEs, oxidative stress and stimulation of TGF- $\beta$ 1 [7,12,54]. Our data also revealed overexpression of renal MMP-2 that could be attributed to the co-expression of TGF $\beta$ -1, AGE-RAGE interaction and associated signaling. The overexpressed MMP-2 mRNA in diabetic rats was downregulated after repeated oral administration of RT, which might be attributed to suppressed RAGE and TGF $\beta$ -1 mRNA expression that led to the downregulation of AGE-RAGE signaling and decreased MMP-2 expression.

NRP-1 has recently gained much attention in DN management [7,16]. Exposure to LDL-AGEs has been reported to suppress the transcription of NRP-1 in renal podocytes and HEK-293 cells, respectively [7]. qRT-PCR analysis revealed downregulation of NRP-1 mRNA expression in diabetic rats, which could be related to enhanced CML and accumulated AGEs in renal tissues. However, RT significantly alleviated NRP-1 expression in the STZ-induced diabetic rats, which might be attributed to the potent inhibitory effects of RT against AGE formation and AGEs-RAGE signaling.

Persistent hyperglycemia, alterations in lipid homeostasis, redox imbalance and accumulation of AGEs influence the development of CKD via increased glomerular hyperpermeability which alters the tight

junctions between renal cells [1,6,9,24]. Our histopathological investigations revealed that persistently elevated blood glucose in experimental diabetic rats resulted in marked changes in renal cytoarchitecture, including abnormal glomerular lobules, enlarged Bowman's space and a lower podocyte count. Treatment with RT markedly attenuated the alterations in renal cytoarchitecture, which may be ascribed to RT-mediated reduction in lipid peroxidation, reduced renal accumulation of lipids and AGEs, improved antioxidant potential and ameliorated AGE-RAGE signaling.

## CONCLUSIONS

The present *in vivo* study revealed that treatment of diabetic rats with RT improved AGE-induced pathologies, affecting biochemical markers of glycaemic control and ASCVD (such as lipids and hepatic HMG-R activity), and circulatory CML and renal fluorogenic AGEs. RT exerted a downregulating effect on RAGE, NF $\kappa$ B-2, TGF- $\beta$ 1 and MMP-2 transcription, and an upregulating effect on NRP-1 expression, which resulted in improved renal ECM and cytomorphology. RT alleviated the circulatory redox imbalance by decreasing CC levels and increasing HDL-associated PON-1 activity. RT exhibited potent antidiabetic and renoprotective effects via the targeting of AGEs and AGE/RAGE-associated signaling, oxidative stress and regulation of NRP-1 expression.

**Funding:** This research was funded by the Research Deanship at University of Hail, Kingdom of Saudi Arabia, Project No. RG-20029.

**Author contributions:** RN and SSA share equal contribution; investigation, writing-original draft; SSA: animal handling, illustrations, writing, reviewing; SA: formal analysis; MK: data curation; AA and SK: editing, statistical analysis; SA: visualization; MSK: conceptualization, supervision and approval of final manuscript.

**Conflict of interest disclosure:** The authors declare no conflict of interest.

## REFERENCES

- Nabi R, Alvi SS, Saeed M, Ahmad S, Khan MS. Glycation and HMG-CoA Reductase Inhibitors: Implication in Diabetes and Associated Complications. *Curr Diabetes Rev.* 2019;15(3):213-23. <https://doi.org/10.2174/1573399814666180924113442>
- Sulaiman MK. Diabetic nephropathy: Recent advances in pathophysiology and challenges in dietary management. *Diabetol Metab Syndr.* 2019;11:7.
- Alicic RZ, Rooney MT, Tuttle KR. Diabetic kidney disease: Challenges, progress, and possibilities. *Clin J Am Soc Nephrol.* 2017;12(12):2032-45. <https://doi.org/10.2215/cjn.11491116>
- Lim AKH. Diabetic nephropathy - Complications and treatment. *Int J Nephrol Renovasc Dis.* 2014;7:361-81.
- Umanath K, Lewis JB. Update on Diabetic Nephropathy: Core Curriculum 2018. *Am J Kidney Dis.* 2018;71(6):884-95. <https://doi.org/10.1053/j.ajkd.2017.10.026>
- Busch M, Franke S, Rüster C, Wolf G. Advanced glycation end-products and the kidney. *Eur J Clin Invest.* 2010;40(8):742-55. <https://doi.org/10.1111/j.1365-2362.2010.02317.x>
- Nabi R, Alvi SS, Shah A, Chaturvedi CP, Iqbal D, Ahmad S, Khan MS. Modulatory role of HMG-CoA reductase inhibitors and ezetimibe on LDL-AGEs-induced ROS generation and RAGE-associated signalling in HEK-293 Cells. *Life Sci.* 2019;235:116823. <https://doi.org/10.1016/j.lfs.2019.116823>
- Manigrasso MB, Juraneck J, Ramasamy R, Schmidt AM. Unlocking the biology of RAGE in diabetic microvascular complications. *Trends Endocrinol Metab.* 2014;25(1):15-22. <https://doi.org/10.1016/j.tem.2013.08.002>
- Chilelli NC, Burlina S, Lapolla A. AGEs, rather than hyperglycemia, are responsible for microvascular complications in diabetes: A "glycoxidation-centric" point of view. *Nutr Metab Cardiovasc Dis.* 2013;23(10):913-9. <https://doi.org/10.1016/j.numecd.2013.04.004>
- Haddad M, Knani I, Bouzidi H, Berriche O, Hammami M, Kerkeni M. Plasma levels of pentosidine, carboxymethyl-lysine, soluble receptor for advanced glycation end products, and metabolic syndrome: The metformin effect. *Dis Markers.* 2016;2016:6248264. <https://doi.org/10.1155/2016/6248264>
- Nabi R, Alvi SS, Khan RH, Ahmad S, Khan MS. Antiglycation study of HMG-R inhibitors and tocotrienol against glycated BSA and LDL: A comparative study. *Int J Biol Macromol.* 2018;116:983-92. <https://doi.org/10.1016/j.ijbiomac.2018.05.115>
- Zakiyanov O, Kalousová M, Zima T, Tesař V. Matrix metalloproteinases in renal diseases: A critical appraisal. *Kidney Blood Press Res.* 2019;44(3):298-330. <https://doi.org/10.1159/000499876>
- Loeffler I, Wolf G. Transforming growth factor- $\beta$  and the progression of renal disease. *Nephrol Dial Transplant.* 2014;29(Suppl 1):i37-i45. <https://doi.org/10.1093/ndt/gft267>
- Zhao L, Zou Y, Liu F. Transforming Growth Factor-Beta1 in Diabetic Kidney Disease. *Front Cell Dev Biol.* 2020;8:187. doi: 10.3389/fcell.2020.00187. <https://doi.org/10.3389/fcell.2020.00187>
- Nabi R, Alvi SS, Shah A, Chaturvedi CP, Faisal M, Alatar AA, Ahmad S, Khan MS. Ezetimibe attenuates experimental diabetes and renal pathologies via targeting the advanced glycation, oxidative stress and AGE-RAGE signalling in rats. *Arch Physiol Biochem.* 2021;1-16. <https://doi.org/10.1080/13813455.2021.1874996>
- Bondeva T, Wolf G. Role of Neuropilin-1 in Diabetic Nephropathy. *J Clin Med.* 2015;4(6):1293-311.
- Alvi SS, Iqbal D, Ahmad S, Khan MS. Molecular rationale delineating the role of lycopene as a potent HMG-CoA

- reductase inhibitor: in vitro and in silico study. *Nat Prod Res.* 2016;30(18):2111-4. <https://doi.org/10.1080/14786419.2015.1108977>
18. Ahmad P, Alvi SS, Iqbal D, Khan MS. Insights into pharmacological mechanisms of polydatin in targeting risk factors-mediated atherosclerosis. *Life Sci.* 2020;254:117756. <https://doi.org/10.1016/j.lfs.2020.117756>
  19. Alvi SS, Ansari IA, Khan I, Iqbal J, Khan MS. Potential role of lycopene in targeting proprotein convertase subtilisin/kexin type-9 to combat hypercholesterolemia. *Free Radic Biol Med.* 2017;108:394-403. <https://doi.org/10.1016/j.freeradbiomed.2017.04.012>
  20. Bolton WK, Catran DC, Williams ME, Adler SG, Appel GB, Cartwright K, Foiles PG, Freedman BI, Raskin P, Ratner RE, Spinowitz BS, Whittier FC, Wuerth JP. Randomized Trial of an Inhibitor of Formation of Advanced Glycation End Products in Diabetic Nephropathy. *Am J Nephrol.* 2004;24(1):32-40. <https://doi.org/10.1159/000075627>
  21. Salunkhe VA, Mollet IG, Ofori JK, Malm HA, Esguerra JLS, Reinbothe TM, Stenkula KG, Wendt A, Eliasson L, Vikman J. Dual Effect of Rosuvastatin on Glucose Homeostasis Through Improved Insulin Sensitivity and Reduced Insulin Secretion. *EBioMedicine.* 2016;10:185-94. <https://doi.org/10.1016/j.ebiom.2016.07.007>
  22. Salunkhe VA, Elvstam O, Eliasson L, Wendt A. Rosuvastatin treatment affects both basal and glucose-induced insulin secretion in INS-1 832/13 cells. *PLoS One.* 2016;11(3):e0151592. <https://doi.org/10.1371/journal.pone.0151592>
  23. Akhter F, Alvi SS, Ahmad P, Iqbal D, Alshehri BM, Khan MS. Therapeutic efficacy of Boerhaavia diffusa (Linn.) root methanolic extract in attenuating streptozotocin-induced diabetes, diabetes-linked hyperlipidemia and oxidative-stress in rats. *Biomed Res Ther.* 2019;6(7):3293-306. <https://doi.org/10.15419/bmrat.v6i7.556>
  24. Hashim A, Alvi SS, Ansari IA, Salman Khan M. Phyllanthus virgatus forst extract and it's partially purified fraction ameliorates oxidative stress and retino-nephropathic architecture in streptozotocin-induced diabetic rats. *Pak J Pharm Sci.* 2019;32(6):2697-708.
  25. Husain I, Akhtar M, Abdin MZ, Islamuddin M, Shaharyar M, Najmi AK. Rosuvastatin ameliorates cognitive impairment in rats fed with high-salt and cholesterol diet via inhibiting acetylcholinesterase activity and amyloid beta peptide aggregation. *Hum Exp Toxicol.* 2018;37(4):399-411. <https://doi.org/10.1177/0960327117705431>
  26. Alvi SS, Ansari IA, Ahmad MK, Iqbal J, Khan MS. Lycopene amends LPS induced oxidative stress and hypertriglyceridemia via modulating PCSK-9 expression and Apo-CIII mediated lipoprotein lipase activity. *Biomed Pharmacother.* 2017;96:1082-93. <https://doi.org/10.1016/j.biopharm.2017.11.116>
  27. Wieland H, Seidel D. A simple specific method for precipitation of low density lipoproteins. *J Lipid Res.* 1983;24(7):904-9. [https://doi.org/10.1016/s0022-2275\(20\)37936-0](https://doi.org/10.1016/s0022-2275(20)37936-0)
  28. Benzie IFF, Strain JJ. The ferric reducing ability of plasma (FRAP) as a measure of "antioxidant power": The FRAP assay. *Anal Biochem.* 1996;239(1):70-6. <https://doi.org/10.1006/abio.1996.0292>
  29. Ayub A, Mackness MI, Arrol S, Mackness B, Patel J, Durrinton PN. Serum Paraoxonase After Myocardial Infarction. *Arterioscler Thromb Vasc Biol.* 1999;19(2):330-5. <https://doi.org/10.1161/01.atv.19.2.330>
  30. Nabi R, Alvi SS, Shah MS, Ahmad S, Faisal M, Alatar AA, Khan MS. A biochemical & biophysical study on in-vitro anti-glycating potential of iridin against D-Ribose modified BSA. *Arch Biochem Biophys.* 2020;686:108373. <https://doi.org/10.1016/j.abb.2020.108373>
  31. Nakagawa T, Yokozawa T, Terasawa K, Nakanishi K. Therapeutic usefulness of Keishi-bukuryo-gan for diabetic nephropathy. *J Pharm Pharmacol.* 2003;55(2):219-27. <https://doi.org/10.1211/002235702450>
  32. Sensi M, Prisci F, Pugliese G, De Rossi MG, Petrucci AFG, Cristina A, Morano S, Pozzessere G, Valle E, Andreani D, Di Mario U. Role of advanced glycation end-products (AGE) in late diabetic complications. *Diabetes Res Clin Pract.* 1995;28(1):9-17. [https://doi.org/10.1016/0168-8227\(94\)01061-4](https://doi.org/10.1016/0168-8227(94)01061-4)
  33. Wang G, Liu Z, Li M, Li Y, Alvi SS, Ansari IA, Khan MS. Ginkgolide B Mediated Alleviation of Inflammatory Cascades and Altered Lipid Metabolism in HUVECs via Targeting PCSK-9 Expression and Functionality. *Biomed Res Int.* 2019;2019:7284767. <https://doi.org/10.1155/2019/7284767>
  34. Alvi SS, Ansari IA, Khan MS. Pleiotropic role of lycopene in protecting various risk factors mediated atherosclerosis. *Ann Phytomedicine.* 2015;4(1):54-60.
  35. Szkudelski T. The mechanism of alloxan and streptozotocin action in B cells of the rat pancreas. *Physiol Res.* 2001;50(6):537-46.
  36. Yazdanimehr S, Mohammadi MT. Protective effects of rosuvastatin against hyperglycemia-induced oxidative damage in the pancreas of streptozotocin-induced diabetic rats. *Physiol Pharmacol.* 2018;22(1):19-27.
  37. Serdar MA, Serteser M, Ucal Y, Karpuzoglu HF, Aksungar FB, Coskun A, Kilercik M, Ünsal İ, Özpinar A. An Assessment of HbA1c in Diabetes Mellitus and Pre-diabetes Diagnosis: a Multi-centered Data Mining Study. *Appl Biochem Biotechnol.* 2020;190(1):44-56. <https://doi.org/10.1007/s12010-019-03080-4>
  38. Dabla PK. Renal function in diabetic nephropathy. *World J Diabetes.* 2010;1(2):48-56.
  39. Mian AN, Schwartz GJ. Measurement and Estimation of Glomerular Filtration Rate in Children. *Adv Chronic Kidney Dis.* 2017;24(6):348-56. <https://doi.org/10.1053/j.ackd.2017.09.011>
  40. Yang H, Song Y, Liang YN, Li R. Quercetin treatment improves renal function and protects the kidney in a rat model of adenine-induced chronic kidney disease. *Med Sci Monit.* 2018;24:4760-6. <https://doi.org/10.12659/msm.909259>
  41. Kiconco R, Rugera SP, Kiwanuka GN. Microalbuminuria and Traditional Serum Biomarkers of Nephropathy among Diabetic Patients at Mbarara Regional Referral Hospital in South Western Uganda. *J Diabetes Res.* 2019; 2019:3534260. <https://doi.org/10.1155/2019/3534260>
  42. Motawi TK, Shehata NI, ElNokeety MM, El-Emady YF. Potential serum biomarkers for early detection of diabetic nephropathy. *Diabetes Res Clin Pract.* 2018;136:150-8. <https://doi.org/10.1016/j.diabres.2017.12.007>

43. Obia O, Chuemere AN, Chike CPR, Nyeche S. Effect of supplementation of natural honey on serum albumin and total protein of alloxan induced diabetic Wistar rats. *Am J Phytomedicine Clin Ther.* 2017;5(3):21.
44. Vergès B. Pathophysiology of diabetic dyslipidaemia: where are we? *Diabetologia.* 2015;58(5):886-99.  
<https://doi.org/10.1007/s00125-015-3525-8>
45. Ahmad P, Alvi SS, Salman Khan M. Functioning of organo-sulfur compounds from garlic (*Allium sativum linn*) in targeting risk factor-mediated atherosclerosis: A cross talk between alternative and modern medicine. In: Akhtar M, Swamy M, Sinniah U, editors. *Natural Bio-active Compounds Vol 1, Production and Applications.* Springer Singapore; 2019. p. 561-85. [https://doi.org/10.1007/978-981-13-7154-7\\_20](https://doi.org/10.1007/978-981-13-7154-7_20)
46. Meneses MJ, Silvestre R, Sousa-Lima I, Macedo MP. Paraoxonase-1 as a regulator of glucose and lipid homeostasis: Impact on the onset and progression of metabolic disorders. *Int J Mol Sci.* 2019;20(16):4049.  
<https://doi.org/10.3390/ijms20164049>
47. Jaouad L, Milochevitch C, Khalil A. PON1 paraoxonase activity is reduced during HDL oxidation and is an indicator of HDL antioxidant capacity. *Free Radic Res.* 2003;37(1):77-83. <https://doi.org/10.1080/1071576021000036614>
48. Ruiz HH, Ramasamy R, Schmidt AM. Advanced glycation end products: Building on the concept of the “common soil” in metabolic disease. *Endocrinology.* 2020;161(1):bqz006.  
<https://doi.org/10.1210/endocr/bqz006>
49. Saulnier PJ, Wheelock KM, Howell S, Weil EJ, Tanamas SK, Knowler WC, Lemley K V, Mauer M, Yee B, Nelson RG, Beisswenger PJ. Advanced glycation end products predict loss of renal function and correlate with lesions of diabetic kidney disease in American Indians with type 2 diabetes. *Diabetes.* 2016;65(12):3744-53.  
<https://doi.org/10.2337/db16-0310>
50. Le Bagge S, Fotheringham AK, Leung SS, Forbes JM. Targeting the receptor for advanced glycation end products (RAGE) in type 1 diabetes. *Med Res Rev.* 2020;40(4):1200-1219. <https://doi.org/10.1002/med.21654>
51. Ott C, Jacobs K, Haucke E, Santos AN, Grune T, Simm A. Role of advanced glycation end products in cellular signaling. *Redox Biol.* 2014;2:411-29.  
<https://doi.org/10.1016/j.redox.2013.12.016>
52. de Medeiros MC, Frasnelli SCT, Bastos A de S, Orrico SRP, Rossa Junior C. Modulation of cell proliferation, survival and gene expression by RAGE and TLR signaling in cells of the innate and adaptive immune response: Role of p38 MAPK and NF-KB. *J Appl Oral Sci.* 2014;22(3):185-93. <https://doi.org/10.1590/1678-775720130593>
53. López-Hernández FJ, López-Novoa JM. Role of TGF- $\beta$  in chronic kidney disease: An integration of tubular, glomerular and vascular effects. *Cell Tissue Res.* 2012;347(1):141-54. <https://doi.org/10.1007/s00441-011-1275-6>
54. Kim ES, Sohn YW, Moon A. TGF- $\beta$ -induced transcriptional activation of MMP-2 is mediated by activating transcription factor (ATF)2 in human breast epithelial cells. *Cancer Lett.* 2007;252(1):147-56.  
<https://doi.org/10.1016/j.canlet.2006.12.016>
55. Alvi SS, Ahmad P, Ishrat M, Iqbal D, Khan MS. Secondary metabolites from rosemary(*Rosmarinus officinalis L.*): Structure, biochemistry and therapeutic implications against neurodegenerative diseases. In: Swamy M, Akhtar M editors. *Natural Bio-active Compounds Vol 2, Chemistry, Pharmacology and Health Care Practices.* Springer Singapore; 2019. p. 1-24. [https://doi.org/10.1007/978-981-13-7205-6\\_1](https://doi.org/10.1007/978-981-13-7205-6_1)

## Supplementary Material

The Supplementary Material is available at: [http://www.serbiosoc.org.rs/NewUploads/Uploads/Nabi%20et%20al\\_6394\\_Supplementary%20Material.pdf](http://www.serbiosoc.org.rs/NewUploads/Uploads/Nabi%20et%20al_6394_Supplementary%20Material.pdf)